Soft Comput (2018) 22:159–176
https://doi.org/10.1007/s00500-016-2319-3

METHODOLOGIES AND APPLICATION

A solution network based on stud krill herd algorithm for optimal power flow problems

Harish Pulluri[1] · **R. Naresh**[1] · **Veena Sharma**[1]

Published online: 24 August 2016

Abstract This paper presents a study based on versatile bio-inspired metaheuristic stud krill herd (SKH) algorithm to tackle the optimal power flow (OPF) problems in a power system network. SKH consists of stud selection and crossover operator that is incorporated into the original krill herd algorithm to improve the quality of the solution and especially to avoid being trapped in local optima. In order to investigate the performance, the proposed algorithm is demonstrated on the optimal power flow problems of IEEE 14-bus, IEEE 30-bus and IEEE 57-bus systems. The different objective functions considered are minimization of total production cost with and without valve point loading effect, minimization of active power loss, minimization of *L*-index and minimization of emission pollution. The OPF results obtained with the proposed approach are compared with the other evolutionary algorithms recently reported in the literature.

Keywords Optimal power flow · Voltage stability · Emission pollution · Evolutionary algorithm · Stud krill herd algorithm

Communicated by V. Loia.

✉ Veena Sharma
veenanaresh@gmail.com

Harish Pulluri
harishpulluri@gmail.com

R. Naresh
rnareshnith@gmail.com

[1] Electrical Engineering Department, National Institute of Technology, Hamirpur, Himachal Pradesh 177005, India

1 Introduction

The power system is a composite and sophisticated system due to its various static/dynamic states, large scale and complex interconnections between different components. Controlling and managing such system is a major challenging issue for system operators. The power flow study can be considered as one of the most significant operating and computing function and hence plays a vital role in power system planning, operation and control. The power flow study is subjected to the various electrical and physical constraints of the power system known as optimal power flow (OPF) problem (Dommel and Tinney 1968). The goal of OPF is to optimize the specific objective functions by adjusting the set of control variables to satisfy the necessary constraints related to the power system network, which include nonlinear power flow equations, load buses voltage magnitudes, the line flows, slack bus active power output and generators reactive power limits. The control variables include generator buses, real power outputs and voltage magnitudes, shunt capacitors and transformer taps connected between various buses. Minimization of total production cost and active power loss is most frequently considered objective functions. However, in some cases, it may be difficult to maintain voltages of the load buses within their limits due to inefficient use of reactive power sources, which may lead to voltage collapse. In those cases, voltage stability enhancement is also considered as one of the objective function. Additionally, due to increased concern regarding environmental protection, minimization of emission pollution is also considered as a part of the OPF problem.

The literature on OPF is considerably large which can be found in Al-Rashidi and El-Hawary (2009), Frank et al. (2012). Many classical methods are used to solve these OPF problems, such as nonlinear programming (Shoults and Sun

1982), linear programming (LP) (Zehar and Sayah 2008), quadratic programming (QP) (Reid and Hasdorf 1973), Newton's algorithm (Sun et al. 1984), interior point (IP) (Torres and Quintana 1998), MATPOWER (Zimmerman et al. 2011), etc. The main disadvantages of these methods include large computational time and sometimes being trapped in local optima. During the recent past, numerous evolutionary algorithms have been introduced to alleviate the limitations of classical methods and provide near globally optimal solution. Lai et al. (1997) solved the optimal power flow problems of IEEE 30-bus system using an improved genetic algorithm (IGA). Vaisakh et al. (2013) developed genetic evolving and direction particle swarm optimization (GEDPSO) by adding ant colony search to classical PSO to enhance its global search ability. Sayah and Zehar (2008) addressed modified differential evolution (MDE) to handle the non-smooth cost function of various test systems. Sinsuphan et al. (2013) suggested improved harmony search algorithm (IHSA) to solve the single-objective OPF problems. In IHSA, Taguchi method is used to enhance the intervals of control variables to attain better initialization and improve the convergence speed of HSA. Ramesh and Premalatha (2015) introduced adaptive real coded biogeography-based optimization (ARCBBO) by adding Gaussian mutation operator into the classical BBO to improve the population diversity. However, these population-based approaches may undergo premature convergence at different stages of search processing. Therefore, efforts toward betterment of the existing optimization techniques and innovation of new computational techniques are needed to solve optimal power flow problems, and the present work is an attempt toward this direction.

The krill herd (KH) algorithm has been first developed by Gandomi and Alavi (2012), and it is inspired by the increasing densities of the krill individuals and reaching high areas of food concentration after predation. The KH algorithm mainly consists of three movements in an iterative process, namely motion induced by the other krill individuals, foraging motion and physical diffusion. Due to the flexibility and efficient characteristics of KH algorithm, researchers have used it fairly for solving different constrained optimization problems (Gai-Ge et al. 2014a, b, c, d, e; Gandomi et al. 2013) successfully. However, the main deficiency of the standard KH algorithm's local search mechanism is that the search process is completely random in nature, and consequently, it may not always find a global optimal solution particularly for high-dimensional practical problems.

Therefore, several variants of KH algorithm are developed such as Gai-Ge et al. (2013, 2014a, b, c, d, e, 2015, 2016), Gaige et al. (2013), Junpeng et al. (2014), Lihong et al. (2014) to improve the local search ability and for solving the optimization problems. Gai-Ge et al. (2014a, b, c, d, e) incorporated a novel migration operator to the KH algorithm for solving optimization problems effectively. Gai-Ge et al. (2013) included concepts of chaotic method and a mutation operator to KH algorithm, which results in improving the exploitation capability of the KH algorithm during run process. To escape the KH from local minima and provide a global solution, Gai-Ge et al. 2014a, b, c, d, e utilized opposition-based concept and Cauchy mutation scheme in the KH algorithm. Gaige et al. (2013) integrated a Leavy flight operator with the KH algorithm to improve the efficiency and convergence speed of KH algorithm in the evolution process.

In this paper, a new bio-inspired algorithm called stud krill herd (SKH) (Gai-Ge et al. 2014a, b, c, d, e) algorithm is proposed and implemented successfully for the first time to solve the OPF problems. Here, krill herd (KH) algorithm is hybridized with a stud genetic algorithm (SGA) (Khatib and Fleming 1998) to reach near-global optimal solution. In the present work, the performance of KH is enhanced by adding an adaptive genetic reproduction mechanism called stud selection and crossover (SSC) operator, which leads to the development of the proposed SKH algorithm. In fact, in SKH algorithm, the search space is explored by first applying KH, and then, the SSC operator is used to take over only the amended possibilities to obtain good solutions. Therefore, the augmented KH algorithm is capable of searching comparatively larger space and extract good OPF solutions. The performance of the algorithm is analyzed and tested on IEEE 14-bus, IEEE 30-bus and IEEE 57-bus systems by considering the different objective function models.

The rest of the paper is organized as follows: Section 2 exhibits the OPF problem formulation, Sect. 3 describes the KH algorithm and proposed SKH algorithm. Solution methodology of the proposed SKH for solving OPF problem is presented in Sect. 4. Section 5 reports the simulation results and conclusions are given in Sect. 6.

2 Optimal power flow problem formulation

The primary function of the OPF problem is to optimize the objective functions by adjusting the control variables while satisfying the set of equality and inequality constraints. The general OPF problem can be formulated as follows:

$$\min f(x, u) \tag{1}$$

$$\text{subject to} \begin{cases} g(x, u) = 0 \\ h(x, u) \leq 0 \end{cases} \tag{2}$$

where f is an objective function to be minimized; x is the vector of state (dependent) variables consisting of slack bus real power generation, load bus voltage magnitudes, reactive power generation at the generator buses and power flows in transmission lines; and u consists of control (independent) variables such as generated buses real power outputs except

slack bus and voltage magnitudes, transformer tap settings and shunt capacitors at the various buses.

2.1 Objective functions

Five different models are considered for different objective functions and are given as follows:

2.1.1 M1 minimization of total production cost

The generation cost function is represented as follows (Ramesh and Premalatha 2015):

$$f_1 = \sum_{k=1}^{\mathrm{NG}} \left(a_k + b_k P_{Gk} + c_k P_{Gk}^2\right) \tag{3}$$

where NG represents number of generator buses; P_{Gk} is the active power generation at kth generating unit; and a_k, b_k, c_k are the cost coefficients of kth generating unit.

2.1.2 M2 minimization of active power loss

Mathematically, the objective function for minimization of active power loss is expressed as follows (Ramesh and Premalatha 2015):

$$f_2 = \sum_{n=1}^{nl} G_n \left(V_k^2 + V_m^2 - 2V_k V_m \cos\theta_{km}\right) \tag{4}$$

where nl represents number of transmission lines; G_n is the conductance of the nth line connected between kth and mth buses; V_k, V_m are the voltage magnitudes at kth and mth buses, respectively; and θ_{km} is the phase angle between kth and mth buses.

2.1.3 M3 minimization of L-index

In a power system network, it is important to maintain the voltages of all load buses within their acceptable limits. However, when the system is subjected to any disturbance, the non-optimized control variables may lead to progressive and large voltage drop leading to voltage collapse in the system. L-index introduced in Kessel and Glavitsch (1986) is used to assess voltage stability margin. Its value at a particular bus indicates the level of closeness of the voltage collapse condition of that bus. Normally, L-index varies from 0 (no-load) to 1 (voltage collapse) condition. Mathematically, the objective function of L-index may be expressed as follows:

$$f_3 = \min(\max(L_k)) \tag{5}$$

where L_k is the L-index of the kth load bus defined as (Kessel and Glavitsch 1986) follows:

$$L_k = \left|1 - \frac{\sum_{m=1}^{\mathrm{NG}} H_{km} V_m}{V_k}\right| \quad \text{where} \quad k = 1, 2, \ldots, \mathrm{LB}; \tag{6}$$

$$H_{km} = -[\mathrm{inv}(Y_{kk})]^*[Y_{km}] \tag{7}$$

where LB represents number of load buses; Y_{kk} is the self-admittance of kth bus; and Y_{km} is the mutual admittance between kth and mth buses.

2.1.4 M4 minimization of emission pollution

Nowadays, society demands not only secure electricity, but also the minimum level of emission pollution discharged by thermal plants. Therefore, emission pollution (EP) is also considered one of the objectives for OPF problem, and it can be expressed as follows (Ramesh and Premalatha 2015):

$$f_4 = \sum_{k=1}^{\mathrm{NG}} \left(\alpha_k + \beta_k P_{Gk} + \gamma_k P_{Gk}^2 + \mu_k \exp\left(\xi_k P_{Gk}\right)\right) \tag{8}$$

where α_k, β_k, γ_k, μ_k, ξ_k are the emission coefficients of kth generating unit.

2.1.5 M5 minimization of total production cost with valve point loading effect

Due to the presence of multiple valves, the large size steam turbine will have wire drawing effects when the steam admission valves start to open. Consequently, the heat rate rises suddenly. This phenomenon is called the valve point loading effect and is represented by adding sinusoidal components to the quadratic total production cost function. Therefore, a non-convex total production cost function is expressed as follows (Vaisakh et al. 2013):

$$f_5 = \sum_{k=1}^{\mathrm{NG}} \left(a_k + b_k P_{Gk} + c_k P_{Gk}^2 + \left|d_k^* \sin\left(e_k^* \left(P_{Gk}^{\min} - P_{Gk}\right)\right)\right|\right) \tag{9}$$

where d_k, e_k are the cost coefficients of additional sinusoidal component of kth generating unit; and $P_{Gk}^{\min}$ is the minimum active power limit of kth generating unit.

2.2 Constraints

The equality constraints $g(x, u)$ are the nonlinear power flow equations, which are expressed as follows:

$$P_{Gk} - P_{Dk} - V_k \sum_{m=1}^{\mathrm{NB}} V_m \left(G_{km} \cos \underset{km}{\theta} + B_{km} \sin \underset{km}{\theta} \right) = 0 \tag{10}$$

$$Q_{Gk} - Q_{Dk} - V_k \sum_{m=1}^{NB} V_m \left(G_{km} \sin \underset{km}{\theta} - B_{km} \cos \underset{km}{\theta} \right) = 0 \tag{11}$$

where P_{Gk}, Q_{Gk} are the active and reactive power generations at kth generating unit, respectively; P_{Dk}, Q_{Dk} are the active and reactive power loads at kth bus, respectively; and G_{km}, B_{km} are the conductance and susceptance between kth and mth buses, respectively.

The inequality constraints $h(x, u)$ are the minimum and maximum limits of independent and dependent variables, which are given as follows:

$$\begin{cases} P_{Gk}^{\min} \le P_{Gk} \le P_{Gk}^{\max} \\ V_{Gk}^{\min} \le V_{Gk} \le V_{Gk}^{\max} \\ Q_{Gk}^{\min} \le Q_{Gk} \le Q_{Gk}^{\max} \end{cases} \quad k = 1, 2, \ldots, \mathrm{NG} \tag{12}$$

$$t_k^{\min} \le t_k \le t_k^{\max} \quad k = 1, 2, \ldots, \mathrm{NT} \tag{13}$$

$$b_{Ck}^{\min} \le b_{Ck} \le b_{Ck}^{\max} \quad k = 1, 2, \ldots, \mathrm{NC} \tag{14}$$

$$V_{Lk}^{\min} \le V_{Lk} \le V_{Lk}^{\max} \quad k = 1, 2, \ldots, \mathrm{LB} \tag{15}$$

$$S_{lk} \le S_{lk}^{\max} \quad k = 1, 2, \ldots, nl \tag{16}$$

where $P_{Gk}^{\min}$, $P_{Gk}^{\max}$ are the minimum and maximum active power limits of the kth generating unit, respectively; $V_{Gk}^{\min}$, $V_{Gk}^{\max}$ are the minimum and maximum voltage limits of the kth generator bus, respectively; V_{Gk} represents voltage at kth generator bus; $Q_{Gk}^{\min}$, $Q_{Gk}^{\max}$ are the minimum and maximum reactive power limits of the kth generating unit, respectively; Q_{Gk} represents reactive power at kth generating unit; $t_k^{\min}$, $t_k^{\max}$ are the minimum and maximum tap settings of the kth transformer tap, respectively; t_k represents tap setting at kth transformer tap; NT represents number of transformer taps; $b_{Ck}^{\min}$, $b_{Ck}^{\max}$ are the minimum and maximum shunt admittance limits of the kth shunt capacitor, respectively; b_{Ck} represents shunt admittance value of kth shunt capacitor; NC represents number of shunt capacitors; $V_{Lk}^{\min}$, $V_{Lk}^{\max}$ are the minimum and maximum voltage limits of the kth load bus, respectively; V_{Lk} represents voltage at kth load bus; and $S_{lk}^{\max}$, S_{lk} are the maximum MVA and MVA flow in kth transmission line.

3 Proposed SKH algorithm

Before understanding the idea behind stud krill herd algorithm, it is necessary to discuss the krill herd algorithm, which is described below.

3.1 Krill herd algorithm

Krill herd (KH) algorithm is a population-based algorithm, which is inspired from the process of increasing densities of the krill individuals and reaching high areas of food concentration after predation. The distance between the food source and highest density of the krill swarm from each krill gives a possible solution. The krill individual, which is closer to the higher krill density and food concentration, represents the best fitness value. Each krill rotates in a multi-dimensional search space, and its positions are modified by three movements in an iterative process namely motion induced by the other krill individuals, foraging motion and physical diffusion and are explained below.

3.1.1 Motion induced by other krill individuals

To reach the high krill density, krill individuals always move in an n-dimensional search space with a certain velocity, and its direction is influenced by the local effect provided by the neighbor krill as well as target effect. Velocity for ith krill is calculated as follows.

$$N_i^q = N^{\max} \underset{i}{\alpha} + \omega_n N_i^{q-1} \tag{17}$$

where,

$$\underset{i}{\alpha} = \alpha_i^{\mathrm{local}} + \overset{\mathrm{target}}{\underset{i}{\alpha}} \tag{18}$$

$$\overset{\mathrm{local}}{\underset{i}{\alpha}} = \sum_{j=1}^{NN} \hat{F}_{ij} \hat{Z}_{ij} \tag{19}$$

$$\hat{Z}_{ij} = \frac{Z_i - Z_j}{\left\| Z_i - Z_j \right\| + \mathrm{rand}} \tag{20}$$

$$\hat{F}_{ij} = \frac{F_i - F_j}{F^{\mathrm{worst}} - F^{\mathrm{best}}} \tag{21}$$

where N_i^q, N_i^{q-1} are the motion induced by other krill individuals to ith krill individual in qth and $(q-1)$th iterations, respectively; $N^{\max}$ represents maximum induced speed; NN represents number of neighbors to each krill individual; ω_n represents inertial weight; $\hat{F}_{ij}$ represents normalized fitness difference between ith and jth krill individuals; $\hat{Z}_{ij}$ represents normalized position difference between ith and jth krill individuals; Z_i, Z_j are the positions of ith and jth krill individuals, respectively; F_i, F_j are the fitness values of ith and jth krill individuals, respectively, and F^{worst}, F^{best} are the worst and best fitness values in all the krill individuals.

In order to find the number of neighbors to each krill individual, sensing distance (d_s) is calculated using Eq. (22) given below. If the distance between any two krill individu-

als is less than the sensing distance, they are considered as neighbors.

$$d_{s,i} = \frac{1}{5^{*}\mathrm{NK}} \left(\sum_{j=1}^{\mathrm{NK}} \| Z_i - Z_j \| \right) \tag{22}$$

where NK represents number of krill individuals; $d_{s,i}$ represents sensing distance of ith krill individual.

$$\overset{\text{target}}{\alpha}_{i} = G^{\text{best}} \hat{F}_{i,\text{best}} \hat{Z}_{i,\text{best}} \tag{23}$$

$$G^{\text{best}} = 2 \left(\text{rand} + q \,/\, q_{\max} \right) \tag{24}$$

where G^{best} represents effective coefficient; $\hat{F}_{\text{i,best}}$ is the normalized fitness difference between ith and best krill individuals; $\hat{Z}_{i,\text{best}}$ represents normalized position difference between ith and best krill individuals; and $q, q_{\max}$ are the current iteration and maximum number of iterations, respectively.

3.1.2 Foraging motion

It consists of two parts, the food location in the current and previous iterations. Good food location is the combination of food attraction, which is used to attract the krill individuals toward the global optimal solution and local best food location. Foraging motion for ith krill is calculated as given below:

$$\mathrm{FM}_i^q = V_{\text{f}} \beta_i + \omega_{\text{f}} \mathrm{FM}_i^{q-1} \tag{25}$$

where,

$$\beta_i = \beta_i^{\text{food}} + \beta_i^{\text{best}} \tag{26}$$

$$\beta_i^{\text{food}} = G^{\text{food}} \hat{Z}_{i,\text{food}} \hat{F}_{i,\text{food}} \tag{27}$$

$$G^{\text{food}} = 2 \left(1 - q \,/\, q_{\max} \right) \tag{28}$$

$$Z^{\text{food}} = \frac{\sum_{i=1}^{\mathrm{NK}} \frac{1}{F_i} Z_i}{\sum_{i=1}^{\mathrm{NK}} \frac{1}{F_i}} \tag{29}$$

$$\beta_i^{\text{best}} = \hat{F}_{i,\text{best}} \hat{Z}_{i,\text{best}} \tag{30}$$

where $\mathrm{FM}_i^q, \mathrm{FM}_i^{q-1}$ are the motion induced by other krill individuals to ith krill individual in qth and $(q-1)$th iterations, respectively; V_{f} represents foraging speed; ω_{f} represents inertia weight constant, between [0, 1]; G^{food} represents food coefficient; Z^{food} represents center of food; $\hat{Z}_{i,\text{food}}$ is the normalized position difference between ith krill and center of food; and $\hat{F}_{i,\text{food}}$ is the normalized fitness difference between ith krill and center of food.

3.1.3 Physical diffusion

When the krill individual moves toward a global optimal solution, it requires less random direction. Therefore, physical diffusion is used in this strategy. It consists of maximum diffusion speed ($D^{\max}$) and random direction vector (δ). δ is used to decrease the random direction of the krill in the iterative process. For ith krill, it is given as follows:

$$D_i^q = (1 - q/q_{\max})\, D^{\max} \delta \tag{31}$$

where D_i^q is the physical diffusion of ith krill individual in qth iteration; $D^{\max}$ represents maximum diffusion speed; and δ represents random directional vector, between $[-1, 1]$.

3.1.4 Update krill position

The position of each krill is updated as follows:

$$Z_i^{q+1} = Z_i^q + C_t \sum_{k=1}^{\mathrm{CV}} (\mathrm{UL}_k - \mathrm{LL}_k) \left(N_i^q + \mathrm{FM}_i^q + D_i^q \right) \tag{32}$$

where Z_i^{q+1}, Z_i^q are the positions of ith krill in $(q+1)$th and qth iterations, respectively; CV represents total number of control variables; C_t represents a random number between [0, 2]; and $\mathrm{UL}_k, \mathrm{LL}_k$ are the upper and lower limits of the kth control variable, respectively.

3.2 Stud krill herd algorithm

The KH algorithm is capable to explore the search space globally, but it fails to select sometimes the global optimum solution in the search space. In order to overcome the problem of KH algorithm and to make this algorithm more efficient, SKH algorithm is developed. In SKH, stud selection and crossover (SSC) operator is used, which accepts the newly generated better solutions only, rather than selecting all the other possible solutions. The idea behind the SSC operator arose from the stud genetic algorithm (SGA), because the selection process in SGA is not completely random. SSC operator mainly consists of two minor operators of SGA viz. selection and crossover. In the selection process, the best krill is selected as the first parent, the second parent is selected to mate with best krill, and then a crossover operator is applied to these two parents to generate a new child krill. Thereafter, fitness value is calculated, and if the fitness value of the child's krill individual is better than the existing individual krill, then it is accepted; otherwise, the krill position is updated by Eq. (32) to be considered in the next generation. Therefore, in the proposed SKH algorithm, first KH is applied to explore thoroughly the search space thereafter

novel SSC operator is employed to take over only the newly generated good solutions. The control scheme of the SSC operator is explained in below mentioned algorithm 1.

Algorithm 1

```
Start
    select the best krill (the stud) for mating
    apply single point crossover to generate a new child krill Z_i'
    evaluate its fitness value F_i'
      if F_i' < F_i^q
          consider the newly generated Z_i' as Z_i^{q+1}
      Else
          update the position of krill individual according to Eq. (32) as Z_i^{q+1}
      End
End
```

4 Proposed SKH algorithm for OPF problems

Stepwise detailed description of the proposed algorithm to solve OPF problems is presented in the following procedure.

Step 1. A krill individual, which represents a complete solution for OPF problems, is randomly initialized. It consists of control variables such as generator buses, real power outputs except slack bus and voltage magnitudes, tap settings of transformers connected between various buses and shunt capacitors, which are randomly generated within their limits. Thus, a krill individual may be expressed as follows:

$$Z_i = \left[P_{Gi,2}, \ldots, P_{Gi,\mathrm{NG}}, V_{Gi,1}, \ldots, V_{Gi,\mathrm{NG}}, t_{i,1}, \ldots, t_{i,\mathrm{NT}}, b_{Ci,1}, \ldots, b_{Ci,\mathrm{NC}}\right] \tag{33}$$

The size of the krill matrix depends upon the number of krill individuals in the population. Each krill in a matrix produces a potential solution to the OPF problems. The complete search space of the SKH algorithm for all krill individuals (NK) is expressed as follows:

$$Z = \begin{bmatrix} Z_1 \\ \vdots \\ Z_i \\ \vdots \\ Z_{\mathrm{NK}} \end{bmatrix} = \begin{bmatrix} P_{\mathrm{G1},2}, \ldots, P_{\mathrm{G1,NG}}, V_{\mathrm{G1},1}, \ldots, V_{\mathrm{G1,NG}}, t_{1,1}, \ldots, t_{1,\mathrm{NT}}, b_{C1,1}, \ldots, b_{C1,\mathrm{NC}} \\ \vdots \\ P_{Gi,2}, \ldots, P_{Gi,\mathrm{NG}}, V_{Gi,1}, \ldots, V_{Gi,\mathrm{NG}}, t_{i,1}, \ldots, t_{i,\mathrm{NT}}, b_{Ci,1}, \ldots, b_{Ci,\mathrm{NC}} \\ \vdots \\ P_{\mathrm{GNK},2}, \ldots, P_{\mathrm{GNK,NG}}, V_{\mathrm{GNK},1}, \ldots, V_{\mathrm{GNK,NG}}, t_{\mathrm{NK},1}, \ldots, t_{\mathrm{NK,NT}}, b_{\mathrm{CNK},1}, \ldots, b_{\mathrm{CNK,NC}} \end{bmatrix} \tag{34}$$

Step 2. The fitness function formulated as a penalty function (Ramesh and Premalatha 2015) is expressed as

$$\begin{aligned} F = f_k &+ w_{\mathrm{P}} \left(\left|\mathrm{P_{G1}}\text{-}\mathrm{P_{G1}^{lim}}\right|\right)^2 \\ &+ w_V \left(\left|V_{Lk} - V_{Lk}^{\lim}\right|\right)^2 + w_Q \left(\left|Q_{Gk} - Q_{Gk}^{\lim}\right|\right)^2 \\ &+ w_S \left(\left|S_{lk} - S_{lk}^{\lim}\right|\right)^2 \end{aligned} \tag{35}$$

where F represents fitness value, f_k is the kth objective function for $k = 1, 2, \ldots, 5$; $\mathrm{P_{G1}}$ represents slack bus active power output; $\mathrm{P_{G1}^{lim}}$, $V_{Lk}^{\lim}$, $Q_{Gk}^{\lim}$, $S_{lk}^{\lim}$ are the minimum or maximum values of the slack bus real power output, load bus voltages, generator reactive power outputs and line flows, respectively, and w_{P}, w_V, w_Q and w_S are the penalty coefficients of the respective constraints. In this work, the values of these coefficients are chosen high in order to eliminate the infeasible krill individuals during the iterative process.

Step 3. Sort all the krill individuals according to their fitness value.

Step 4. Compute three motions namely motion induced by the other kill individual, foraging motion and physical diffusion using Eqs. (17), (25) and (31), respectively, to each krill.

Step 5. Update the position of each krill using Algorithm 1.

Step 6. If any control variable x_i is violated, then it is handled as expressed below:

$$x_i = \begin{cases} x_{\max}, & \text{if} \quad x_i > x_{\max} \\ x_{\min}, & \text{else if} \quad x_i < x_{\min} \end{cases} \tag{36}$$

Step 7. If the maximum number of iterations is reached, then stop the procedure and print the optimum schedule, otherwise go to Step 3.

The flowchart of the proposed method for solving OPF problem is depicted in Fig. 1.

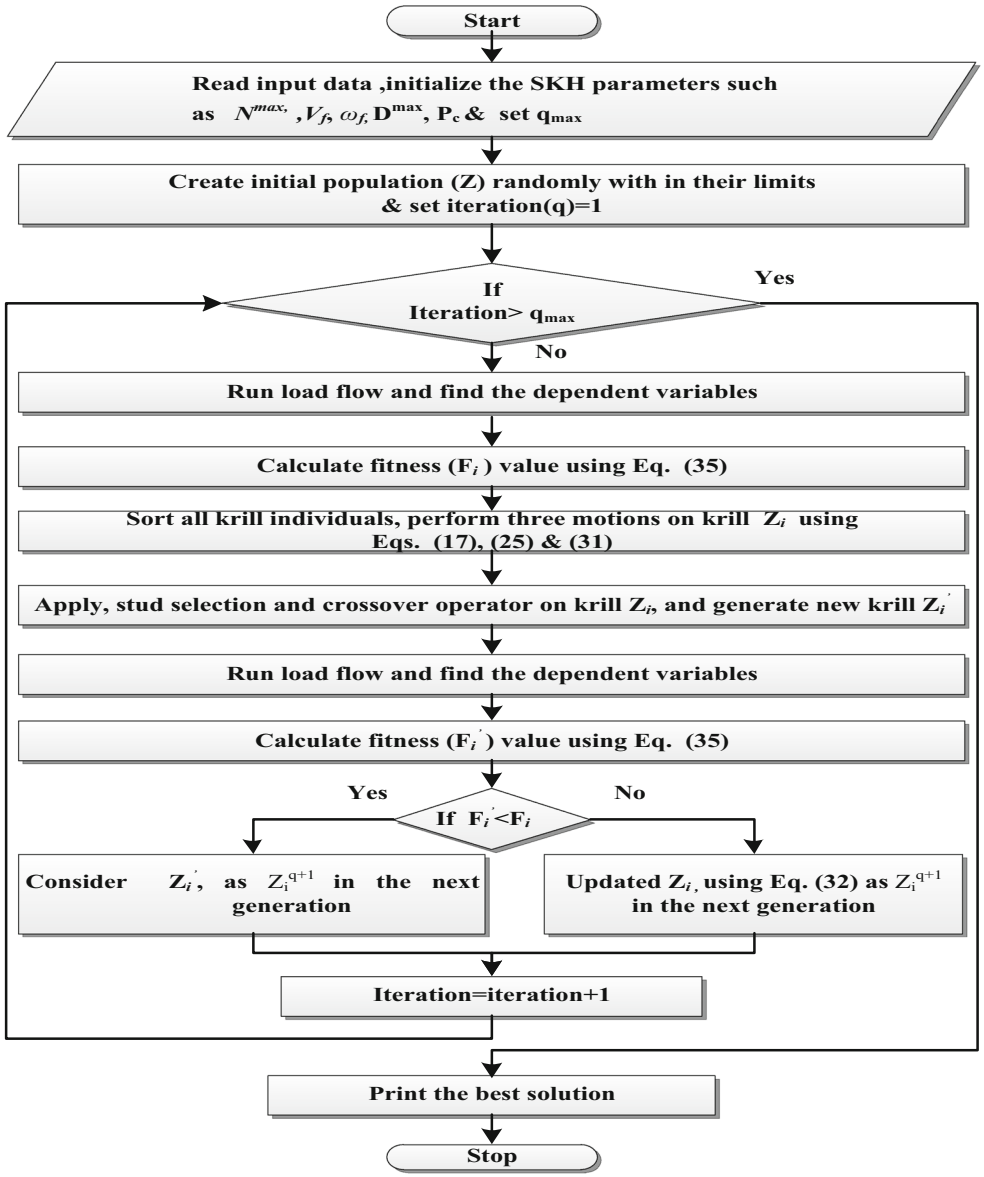

Fig. 1 Flowchart of the proposed SKH algorithm

5 Simulation results

In order to examine the effectiveness of the proposed algorithm, IEEE 14-bus, IEEE 30-bus and IEEE 57-bus systems are considered for solving OPF problems with the same objective functions as considered in Ramesh and Premalatha (2016). The proposed simulation work was implemented on a 2.2 GHz, i3 core processor with MATLAB 2009a. The population size has been taken as 60, and the maximum number of iterations is set to 200 for these test systems.

5.1 IEEE 14-bus system (Test system 1)

To test the feasibility of the proposed SKH algorithm, initially, IEEE 14-bus system is considered which comprises of 20 transmission lines and system real power demand is 259 MW. It has thirteen control variables, which include four generators active powers, five generators voltages, three transformer taps and one shunt capacitor. The minimum and maximum voltages of all the buses lie between 0.94 and 1.06 p.u. The transformer taps are considered between 0.9 and 1.1 p.u., and shunt capacitors lie between 0 and 0.05 p.u. Detailed information about IEEE 14-bus system and generator cost coefficients are considered from Zimmerman et al. (2011); emission coefficients are referred from Sarat and Sudhansu (2015), and for fair comparison, the generator cost coefficients for model 5 (M5) are considered from Belgin and Rengin (2013).

Table 1 Effect of control parameters of SKH method on minimum total production cost over 20 trials for IEEE 14-bus system

Input parameters		TPC ($/h)	Input parameters		TPC ($/h)	Input parameters		TPC ($/h)	Input parameters		TPC ($/h)	Input parameters		TPC ($/h)
N_{max}	V_f		N_{max}	V_f		N_{max}	V_f		N_{max}	V_f		N_{max}	V_f	
$D^{max} = 0.005$; Single-point crossover ($P_c = 1$)														
0.005	0.01	8086.050	0.005	0.02	8084.572	0.005	0.03	8084.188	0.005	0.04	8083.293	0.005	0.05	8085.673
0.01	0.01	8085.162	0.01	0.02	8084.851	0.01	0.03	8083.622	0.01	0.04	8083.154	0.01	0.05	8084.821
0.02	0.01	8084.338	0.02	0.02	8083.638	0.02	0.03	8082.780	0.02	0.04	8083.487	0.02	0.05	8084.133
0.03	0.01	8083.569	0.03	0.02	8082.602	0.03	0.03	8081.591	0.03	0.04	8082.185	0.03	0.05	8083.100
0.04	0.01	8082.570	0.04	0.02	8081.356	**0.04**	**0.03**	**8080.704**	0.04	0.04	8081.222	0.04	0.05	8081.899
0.05	0.01	8082.920	0.05	0.02	8082.099	0.05	0.03	8081.393	0.05	0.04	8082.838	0.05	0.05	8083.059
$D^{max} = 0.01$; Single-point crossover ($P_c = 1$)														
0.005	0.01	8086.791	0.005	0.02	8085.535	0.005	0.03	8084.854	0.005	0.04	8083.572	0.005	0.05	8086.082
0.01	0.01	8086.077	0.01	0.02	8084.827	0.01	0.03	8083.067	0.01	0.04	8084.317	0.01	0.05	8085.303
0.02	0.01	8085.362	0.02	0.02	8084.879	0.02	0.03	8083.812	0.02	0.04	8084.039	0.02	0.05	8085.086
0.03	0.01	8084.740	0.03	0.02	8083.879	0.03	0.03	8083.151	0.03	0.04	8083.570	0.03	0.05	8084.572
0.04	0.01	8083.834	0.04	0.02	8082.941	0.04	0.03	8081.426	0.04	0.04	8082.613	0.04	0.05	8083.388
0.05	0.01	8084.216	0.05	0.02	8083.355	0.05	0.03	8082.703	0.05	0.04	8083.230	0.05	0.05	8083.988
$D^{max} = 0.005$; Two-point crossover ($P_c = 1$)														
0.005	0.01	8087.786	0.005	0.02	8086.585	0.005	0.03	8085.620	0.005	0.04	8086.301	0.005	0.05	8087.416
0.01	0.01	8087.073	0.01	0.02	8086.183	0.01	0.03	8084.853	0.01	0.04	8085.714	0.01	0.05	8086.896
0.02	0.01	8086.292	0.02	0.02	8085.019	0.02	0.03	8084.338	0.02	0.04	8085.142	0.02	0.05	8086.193
0.03	0.01	8085.612	0.03	0.02	8084.662	0.03	0.03	8083.067	0.03	0.04	8084.230	0.03	0.05	8085.511
0.04	0.01	8085.169	0.04	0.02	8084.007	0.04	0.03	8082.716	0.04	0.04	8083.436	0.04	0.05	8084.759
0.05	0.01	8086.171	0.05	0.02	8085.324	0.05	0.03	8083.887	0.05	0.04	8084.464	0.05	0.05	8085.262
$D^{max} = 0.01$; Two-point crossover ($P_c = 1$)														
0.005	0.01	8089.316	0.005	0.02	8087.873	0.005	0.03	8086.291	0.005	0.04	8087.375	0.005	0.05	8088.765
0.01	0.01	8088.582	0.01	0.02	8087.206	0.01	0.03	8085.263	0.01	0.04	8086.954	0.01	0.05	8087.446
0.02	0.01	8086.791	0.02	0.02	8085.275	0.02	0.03	8084.283	0.02	0.04	8084.930	0.02	0.05	8085.690
0.03	0.01	8085.912	0.03	0.02	8085.222	0.03	0.03	8083.268	0.03	0.04	8084.651	0.03	0.05	8086.115
0.04	0.01	8084.427	0.04	0.02	8083.502	0.04	0.03	8081.831	0.04	0.04	8082.180	0.04	0.05	8084.543
0.05	0.01	8086.189	0.05	0.02	8084.182	0.05	0.03	8083.154	0.05	0.04	8084.618	0.05	0.05	8085.982

Bold values indicate the selection of optimal parameters at minimum total production cost

Table 2 Comparison of statistical results with other methods for IEEE 14-bus system

Different models	Method	Minimum	Average	Worst	SD	ET(s)
M1	**SKH**	**8080.7045**	**8081.4451**	**8083.0272**	**0.6697**	**8.56**
	KH	**8081.9462**	**8083.8741**	**8086.5605**	**1.5938**	**7.84**
	MATPOWER (Zimmerman et al. 2011)	8081.53	–	–	–	–
M2	**SKH**	**0.6037**	**0.6760**	**0.8165**	**0.0700**	**8.95**
	KH	**0.6532**	**0.7846**	**1.1006**	**0.1238**	**8.02**
M3	**SKH**	**0.0750**	**0.0757**	**0.0775**	**0.0008**	**8.21**
	KH	**0.0755**	**0.0769**	**0.0782**	**0.0009**	**7.43**
M4	**SKH**	**0.1612**	**0.1617**	**0.1624**	**0.0004**	**8.78**
	KH	**0.1616**	**0.1623**	**0.1646**	**0.0008**	**7.93**
M5	**SKH**	**833.2036**	**833.5976**	**834.6479**	**0.4382**	**9.12**
	KH	**834.1719**	**835.1492**	**836.2631**	**0.7001**	**8.43**
	PSO (Belgin and Rengin 2013)	833.57	–	–	–	–
	SFLA-SA (Belgin and Rengin 2013)	834.36	–	–	–	–
	PSO (Celal and Serdar 2011)	836.45	–	–	–	–
	MSG-HS (Celal and Serdar 2011)	896.68	–	–	–	–
	HGA (Belgin and Rengin 2013)	905.54	–	–	–	–

Shuffled frog leaping algorithm–simulated annealing (SFLA-SA); modified subgradient–harmony search (MSG-HS); hybrid genetic algorithm (HGA).
(–) in above table represents that the results are not available in the literature

Table 3 Optimal control variables for all models of IEEE 14-bus system

Control variables	M1	M2	M3	M4	M5
P_{G1}(MW)	194.4830	8.5648	10.9645	109.1501	199.6102
P_{G2}(MW)	36.3859	21.8190	103.0485	48.1776	20.0009
P_{G3}(MW)	29.7104	89.1289	96.4996	39.1971	21.3076
P_{G6}(MW)	0.1031	40.0908	0.000	32.5855	16.0224
P_{G8}(MW)	7.5717	100.0000	50.4486	34.2249	11.3568
V_{G1}(p.u.)	1.0599	1.0600	1.0600	1.0484	1.0600
V_{G2}(p.u.)	1.0392	1.0554	1.0600	1.0351	1.0438
V_{G3}(p.u.)	1.0140	1.0532	1.0596	1.0105	1.0209
V_{G6}(p.u.)	1.0253	1.0450	1.0600	1.0600	1.0184
V_{G8}(p.u.)	1.0599	1.0600	1.0600	1.0415	1.0567
t_{4-7}(p.u.)	1.0309	0.9956	0.9781	0.9000	1.0221
t_{4-9}(p.u.)	0.9000	0.9237	0.9000	1.0304	0.9329
t_{5-6}(p.u.)	1.0021	1.0014	0.9743	0.9504	1.0175
b_{C9}(p.u.)	0.0497	0.0344	0.0500	0.0500	0.0210
TPC ($/h)	**8080.7045**	10094.15	10936.69	8517.473	**833.2036**
APL (MW)	9.2543	**0.6037**	1.9614	4.3355	9.2981
L-index	0.0803	0.0779	**0.0750**	0.0778	0.0827
EP (ton/h)	0.2364	0.3368	0.3205	**0.1612**	0.2375

The values of the tuning parameters used in SKH algorithm, namely maximum induced speed ($N^{\max}$), diffusion speed ($D^{\max}$), foraging speed (V_f) and type of crossover are required to be selected judiciously. For the tuning of these parameters, twenty independent trials were run with different values of $N^{\max}$, $D^{\max}$, V_f with single- and two-point crossover operators for M1 and are mentioned in Table 1. From this table, it is identified that the single-point crossover gives better results compared to two-point crossover. The optimal value of TPC 8080.704 ($/h) is obtained with $N^{\max} = 0.04$, $D^{\max} = 0.03$ and $V_f = 0.005$ with single-point crossover. Hence, for further investigations of objective models $N^{\max} = 0.04$, $D^{\max} = 0.03$ and $V_f = 0.005$ with single-point crossover are used. The inertia weights are set to 0.9 initially and later decreased linearly up to 0.1.

Both KH and the proposed SKH algorithms have been applied to solve all the objective function models mentioned in Sect. 2.1. With the selected SKH parameters, the minimum, the average, the maximum objective function values, along with standard deviation (SD) and execution time (ET) of 200 generations over 20 trials are compared with the other methods presented in the literature and are reported in Table 2, from where it is inferred that the proposed SKH algorithm provides better overall statistical results in reasonable computational time. The best combination of control parameters attained with SKH algorithm along with the total production cost with and without valve point lading effect, active power loss, L-index and emission pollution for all the models are mentioned in Table 3. The minimum and maximum load voltages attained in all the models are depicted in Fig. 2, which proves that the SKH algorithm is capable to handle all the voltage constraints within their limits. The convergence characteristics obtained using KH and SKH algorithms are plotted in Fig. 3 for objective function M1 from where it is seen that both the algorithms are converging efficiently, but SKH algorithm quickly brings down the objective function to optimal value as compared to KH algorithm.

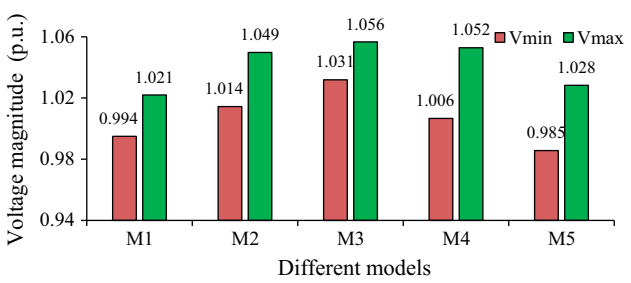

Fig. 2 Minimum and maximum load bus voltages of various models for IEEE 14-bus system

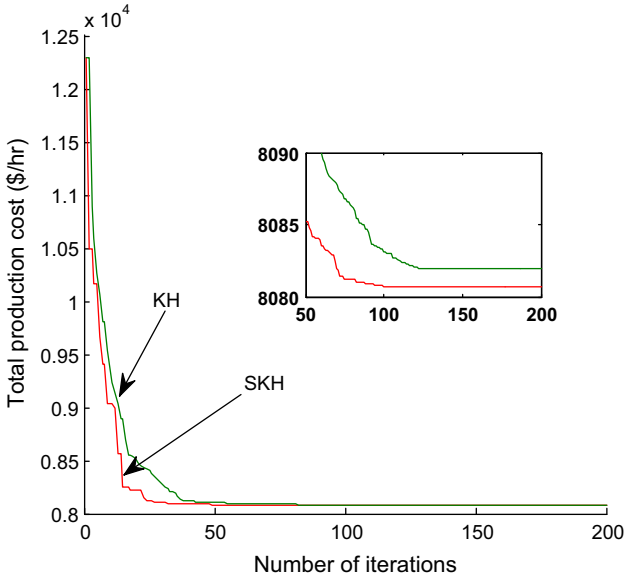

Fig. 3 Convergence characteristics with KH and SKH algorithms of M1 for IEEE 14-bus system

5.2 IEEE 30-bus system (Test system 2)

The test system consists of six generators, 41 branches, and the system real power demand is 283.4 MW. It has 24 control variables, which include five unit active power outputs, six generators voltage magnitudes, four transformer taps and nine shunt branch capacitors. Voltage magnitudes of the generator buses are considered between [0.95, 1.1] p.u. The transformer taps are considered in the range between [0.9, 1.1] p.u. The load buses voltage magnitudes are considered in the range of [0.95, 1.05] p.u. The shunt capacitor values are lie between [0, 0.05] p.u. The information about the bus data, branch data and fuel cost coefficients have been taken from Ramesh and Premalatha (2015).

To obtain the optimal combination of tuning parameters for IEEE 30-bus system, the minimum total production cost value over 20 independent trials with different combination of $N^{\max}$, $D^{\max}$, V_f, for single- and two-point crossover operators are calculated and details are mentioned in Table 4. From this table, it is identified that the single-point crossover gives better results compared with two-point crossover, and the optimal combination of these parameters to get the best performance of the proposed algorithm is $N^{\max} = 0.04$, $V_f = 0.03$, $D^{\max} = 0.005$ with single-point crossover. The inertia weights ω_n and ω_f are set to 0.9 initially and later decreased linearly up to 0.1.

The IEEE 30-bus system has been solved with both KH and proposed SKH algorithms. With the selected SKH parameters, the minimum, the average, the worst values, the standard deviation (SD) and the execution time (ET) for the objective function models, M1 to M5 over 20 trials, are

Table 4 Effect of control parameters of SKH method on minimum total production cost over 20 trials for IEEE 30-bus system

Input parameters		TPC ($/h)	Input parameters		TPC ($/h)	Input parameters		TPC ($/h)	Input parameters		TPC ($/h)	Input parameters		TPC ($/h)
N_{max}	V_f		N_{max}	V_f		N_{max}	V_f		N_{max}	V_f		N_{max}	V_f	
$D^{max} = 0.005$; Single-point crossover ($P_c = 1$)														
0.005	0.01	800.7483	0.005	0.02	800.7093	0.005	0.03	800.6879	0.005	0.04	800.7160	0.005	0.05	800.7213
0.01	0.01	800.6691	0.01	0.02	800.6493	0.01	0.03	800.6478	0.01	0.04	800.6526	0.01	0.05	800.6572
0.02	0.01	800.6364	0.02	0.02	800.6203	0.02	0.03	800.5597	0.02	0.04	800.5820	0.02	0.05	800.6301
0.03	0.01	800.5710	0.03	0.02	800.5506	0.03	0.03	800.5211	0.03	0.04	800.5344	0.03	0.05	800.5409
0.04	0.01	800.5393	0.04	0.02	800.5194	**0.04**	**0.03**	**800.5141**	0.04	0.04	800.5213	0.04	0.05	800.5333
0.05	0.01	800.5882	0.05	0.02	800.5460	0.05	0.03	800.5186	0.05	0.04	800.5261	0.05	0.05	800.5319
$D^{max} = 0.01$; Single-point crossover ($P_c = 1$)														
0.005	0.01	800.7902	0.005	0.02	800.7462	0.005	0.03	800.6793	0.005	0.04	800.6685	0.005	0.05	800.7015
0.01	0.01	800.6841	0.01	0.02	800.6490	0.01	0.03	800.6012	0.01	0.04	800.6321	0.01	0.05	800.6670
0.02	0.01	800.6160	0.02	0.02	800.5778	0.02	0.03	800.5664	0.02	0.04	800.5801	0.02	0.05	800.6472
0.03	0.01	800.5813	0.03	0.02	800.5662	0.03	0.03	800.5460	0.03	0.04	800.5568	0.03	0.05	800.5788
0.04	0.01	800.5595	0.04	0.02	800.5402	0.04	0.03	800.5292	0.04	0.04	800.5353	0.04	0.05	800.5489
0.05	0.01	800.5725	0.05	0.02	800.5648	0.05	0.03	800.5352	0.05	0.04	800.5490	0.05	0.05	800.5678
$D^{max} = 0.005$; Two-point crossover ($P_c = 1$)														
0.005	0.01	800.9755	0.005	0.02	800.8948	0.005	0.03	800.7714	0.005	0.04	800.8076	0.005	0.05	800.8883
0.01	0.01	800.8362	0.01	0.02	800.7943	0.01	0.03	800.7903	0.01	0.04	800.7792	0.01	0.05	800.7824
0.02	0.01	800.7837	0.02	0.02	800.7380	0.02	0.03	800.7255	0.02	0.04	800.7388	0.02	0.05	800.7829
0.03	0.01	800.7213	0.03	0.02	800.6902	0.03	0.03	800.6520	0.03	0.04	800.5826	0.03	0.05	800.6371
0.04	0.01	800.6451	0.04	0.02	800.6042	0.04	0.03	800.5802	0.04	0.04	800.5917	0.04	0.05	800.5854
0.05	0.01	800.6744	0.05	0.02	800.6441	0.05	0.03	800.5917	0.05	0.04	800.6310	0.05	0.05	800.6685
$D^{max} = 0.01$; Two point crossover ($P_c = 1$)														
0.005	0.01	801.8131	0.005	0.02	801.4442	0.005	0.03	801.2084	0.005	0.04	800.9877	0.005	0.05	801.9874
0.01	0.01	801.6284	0.01	0.02	801.2021	0.01	0.03	801.1198	0.01	0.04	801.1278	0.01	0.05	801.1433
0.02	0.01	801.3115	0.02	0.02	801.1400	0.02	0.03	800.9950	0.02	0.04	801.0068	0.02	0.05	801.0137
0.03	0.01	801.0480	0.03	0.02	800.9824	0.03	0.03	800.8111	0.03	0.04	800.9256	0.03	0.05	800.9648
0.04	0.01	800.9169	0.04	0.02	800.8131	0.04	0.03	800.7026	0.04	0.04	800.8131	0.04	0.05	800.9269
0.05	0.01	800.9502	0.05	0.02	800.9425	0.05	0.03	800.8844	0.05	0.04	800.9738	0.05	0.05	801.0435

Bold values indicate the selection of optimal parameters at minimum total production cost

Table 5 Comparison of statistical results with other methods for IEEE 30-bus system

Different models	Method	Minimum	Average	Worst	SD	ET(s)
M1	**SKH**	**800.5141**	**800.6299**	**800.8762**	**0.0944**	**18.23**
	KH	**800.8013**	**800.9255**	**801.1915**	**0.1055**	**16.63**
	ARCBBO (Ramesh and Premalatha 2015)	800.5159	800.6412	800.9262	–	–
	ABC (Rezaei Adaryani and Karami 2013)	800.6600	800.8715	801.8674	–	–
	LDI-PSO (Rezaei Adaryani and Karami 2013)	800.7398	801.5576	803.8698	–	–
	IGA (Lai et al. 1997)	800.805	–	–	–	–
	RCBBO (Ramesh and Premalatha 2015)	800.8703	802.02	802.9431	–	–
	BBO (Ramesh and Premalatha 2015)	801.0562	801.7414	802.4174	–	–
M2	**SKH**	**3.0987**	**3.1116**	**3.1878**	**0.0181**	**18.89**
	KH	**3.1100**	**3.1630**	**3.2413**	**0.0349**	**16.92**
	ARCBBO (Ramesh and Premalatha 2015)	3.1009	3.1156	3.1817	–	–
	ABC (Rezaei Adaryani and Karami 2013)	3.1078	–	–	–	–
	EGA (Sailaja Kunari and Maheswarapu 2010)	3.2008	–	–	–	–
M3	**SKH**	**0.1366**	**0.1372**	**0.1384**	**0.0006**	**19.01**
	KH	**0.1368**	**0.1379**	**0.1391**	**0.0007**	**16.98**
	ARCBBO (Ramesh and Premalatha 2015)	0.1369	0.1375	0.1387	–	–
	ABC (Rezaei Adaryani and Karami 2013)	0.1379	0.1960	0.7201	–	–
M4	**SKH**	**0.2048**	**0.2049**	**0.2051**	**0.0000**	**18.02**
	KH	**0.2049**	**0.2050**	**0.2054**	**0.0001**	**16.54**
	ARCBBO (Ramesh and Premalatha 2015)	0.2048	0.2054	0.2064	–	–
	ABC (Rezaei Adaryani and Karami 2013)	0.204826	–	–	–	–
M5	**SKH**	**930.6598**	**930.8719**	**931.2666**	**0.2041**	**19.56**
	KH	**931.0440**	**931.4664**	**932.1483**	**0.3262**	**17.23**
	GEADPSO (Vaisakh et al. 2013)	930.7454	–	–	–	–
	MDE (Sayah et al. 2008)	930.7930	–	–	–	–

Linearly decreasing inertia PSO (LDI-PSO); enhanced GA (EGA); modified DE (MDE).

reported in Table 5. From this table, it is observed that the SKH algorithm obtained better optimal values compared to the other methods considered in this work. The optimal control variables computed using SKH along with the minimum total production cost (TPC) with and without valve point loading effect, active power loss (APL), L-index and emission pollution (EP) obtained are shown in Table 6 for all the objective models, M1 to M5 considered in this study. The minimum and maximum load bus voltage magnitudes obtained from all the objective function models shown in Fig. 4 confirm the compliance of voltage inequality constraints at all the load buses. The L-index values computed using SKH algorithm for objective models, M1 and M3, are 0.1382 and 0.1366, from which it can be perceived that the L-index value obtained for M3 lesser by 1.36 % in comparison with M1. Therefore, voltage stability is improved. Figure 5 illustrates the convergence characteristics attained using KH and SKH algorithms, from where it is observed that the SKH algorithm has fast convergence characteristics compared to KH algorithm.

5.3 IEEE 57-bus system (Test system 3)

The test system comprises of seven generators, 80 branch lines and 50 load buses. System real power demand is 1266.42 MW, and it has 33 control variables, in which six generators active power outputs, seven generator buses voltage magnitudes, seventeen transformer taps within the range of [0.9, 1.1] p.u., and three shut capacitors are lie between [0, .3] p.u. The voltage magnitudes of all the buses are considered in the interval [0.94, 1.06] p.u. The bus data, fuel cost coefficients and branch data are referred from Zimmerman et al. (2011).

For IEEE 57-bus system, the minimum total production cost value over 20 independent trials with different values of $N^{\max}$, $D^{\max}$, V_{f}, for single- and two-point crossover are mentioned in Table 7. It is observed that the single-point crossover gives better results compared with two-point crossover, and the optimal combination of these parameters to get the better performance of the proposed algorithm are $N^{\max} = 0.05$, $V_{\mathrm{f}} = 0.03$, $D^{\max} = 0.01$ with single-point crossover. The

Table 6 Optimal control variables for all models of IEEE 30-bus system

Control variables	M1	M2	M3	M4	M5
P_{G1}(MW)	177.1421	51.4987	180.6225	64.0619	197.6693
P_{G2}(MW)	48.6393	80.0000	44.8154	67.5706	52.0570
P_{G5}(MW)	21.3132	49.9999	15.8477	49.9999	15.0000
P_{G8}(MW)	21.2568	34.9999	10.2037	35.0000	10.0000
P_{G11}(MW)	11.9684	30.0000	29.8161	30.0000	10.0000
P_{G13}(MW)	12.0000	40.0000	12.0000	40.0000	12.0000
V_{G1}(p.u.)	1.0844	1.0613	1.0752	1.0630	1.0421
V_{G2}(p.u.)	1.0648	1.0572	1.0650	1.0569	1.0190
V_{G5}(p.u.)	1.0332	1.0378	1.0686	1.0374	0.9659
V_{G8}(p.u.)	1.0378	1.0441	1.0564	1.0439	1.0429
V_{G11}(p.u.)	1.0818	1.0663	1.1000	1.0827	1.1000
V_{G13}(p.u.)	1.0460	1.0537	1.0304	1.0527	1.1000
t_{6-9}(p.u.)	1.0105	1.0439	1.0429	1.0252	1.0999
t_{6-10}(p.u.)	0.9785	0.9308	0.9000	0.9510	1.1000
t_{4-12}(p.u.)	0.9651	0.9919	0.9362	0.9880	1.0999
t_{28-27}(p.u.)	0.9733	0.9761	0.9637	0.9758	1.0720
b_{C10}(p.u.)	0.0375	0.0327	0.0087	0.0000	0.0499
b_{C12}(p.u.)	0.0046	0.0238	0.0046	0.0129	0.0499
b_{C15}(p.u.)	0.0388	0.0415	0.0480	0.0442	0.0500
b_{C17}(p.u.)	0.0499	0.0499	0.0258	0.0499	0.0499
b_{C20}(p.u.)	0.0404	0.0392	0.0000	0.0387	0.0500
b_{C21}(p.u.)	0.0500	0.0500	0.0002	0.0500	0.0499
b_{C23}(p.u.)	0.0288	0.0287	0.0095	0.0291	0.0499
b_{C24}(p.u.)	0.0499	0.0499	0.0007	0.0500	0.0499
b_{C29}(p.u.)	0.0236	0.0224	0.0000	0.0218	0.0235
TPC ($/h)	**800.5141**	967.6594	814.0100	944.3802	**930.6598**
APL (MW)	9.0282	**3.0987**	9.9056	3.2326	13.3263
L-index	0.1382	0.1385	**0.1366**	0.1384	0.1568
EP (ton/h)	0.3662	0.2072	0.3740	**0.2048**	0.4353

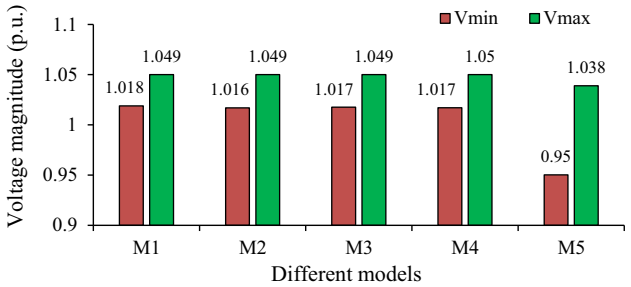

Fig. 4 Minimum and maximum load bus voltages of various models for IEEE 30-bus system

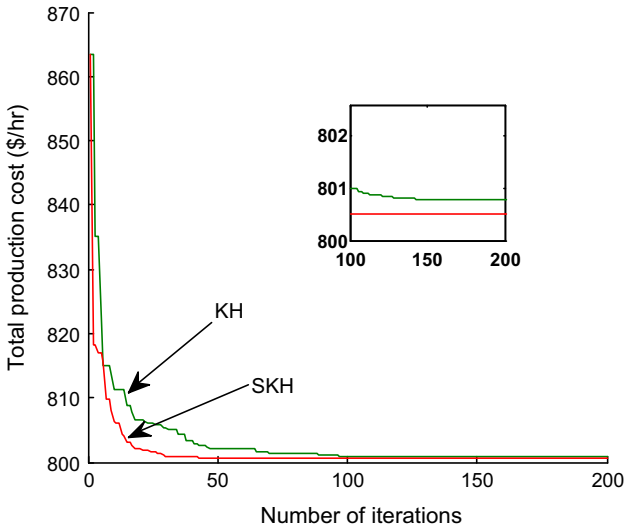

Fig. 5 Convergence characteristics with KH and SKH algorithms of M1 for IEEE 30-bus system

inertia weights ω_n and ω_f are set to 0.9 initially and later decreased linearly up to 0.1.

The proposed SKH algorithm has been implemented for solving different objective function models mentioned in problem formulation. Table 8 shows the minimum, the average, the worst values, the SD and the ET obtained for the

Table 7 Effect of control parameters of SKH method on minimum total production cost over 20 trials for IEEE 57-bus system

Input parameters		TPC ($/h)	Input parameters		TPC ($/h)	Input parameters		TPC ($/h)	Input parameters		TPC ($/h)	Input parameters		TPC ($/h)
N_{max}	V_f		N_{max}	V_f		N_{max}	V_f		N_{max}	V_f		N_{max}	V_f	
$D^{max} = 0.005$; Single-point crossover ($P_c = 1$)														
0.005	0.01	41707.83	0.005	0.02	41705.76	0.005	0.03	41704.02	0.005	0.04	41706.93	0.005	0.05	41710.37
0.01	0.01	41706.10	0.01	0.02	41704.92	0.01	0.03	41702.41	0.01	0.04	41705.93	0.01	0.05	41708.04
0.02	0.01	41707.82	0.02	0.02	41704.76	0.02	0.03	41700.23	0.02	0.04	41703.63	0.02	0.05	41705.98
0.03	0.01	41705.19	0.03	0.02	41702.92	0.03	0.03	41699.20	0.03	0.04	41701.18	0.03	0.05	41703.19
0.04	0.01	41702.79	0.04	0.02	41700.05	0.04	0.03	41697.95	0.04	0.04	41699.54	0.04	0.05	41703.35
0.05	0.01	41698.67	0.05	0.02	41696.08	0.05	0.03	41695.23	0.05	0.04	41697.38	0.05	0.05	41700.27
$D^{max} = 0.01$; Single-point crossover ($P_c = 1$)														
0.005	0.01	41700.20	0.005	0.02	41697.98	0.005	0.03	41695.69	0.005	0.04	41696.42	0.005	0.05	41698.70
0.01	0.01	41696.81	0.01	0.02	41692.62	0.01	0.03	41690.56	0.01	0.04	41693.45	0.01	0.05	41694.64
0.02	0.01	41693.28	0.02	0.02	41690.25	0.02	0.03	41689.67	0.02	0.04	41687.38	0.02	0.05	41690.54
0.03	0.01	41688.81	0.03	0.02	41684.33	0.03	0.03	41688.39	0.03	0.04	41683.69	0.03	0.05	41686.29
0.04	0.01	41684.78	0.04	0.02	41682.10	0.04	0.03	41678.93	0.04	0.04	41680.04	0.04	0.05	41683.39
0.05	0.01	41682.06	0.05	0.02	41679.09	**0.05**	**0.03**	**41676.91**	0.05	0.04	41677.87	0.05	0.05	41680.26
$D^{max} = 0.005$; Two-point crossover ($P_c = 1$)														
0.005	0.01	41706.72	0.005	0.02	41703.41	0.005	0.03	41702.50	0.005	0.04	41700.83	0.005	0.05	41702.91
0.01	0.01	41708.20	0.01	0.02	41704.06	0.01	0.03	41701.98	0.01	0.04	41699.83	0.01	0.05	41703.06
0.02	0.01	41704.65	0.02	0.02	41702.85	0.02	0.03	41698.71	0.02	0.04	41699.42	0.02	0.05	41702.48
0.03	0.01	41698.50	0.03	0.02	41696.43	0.03	0.03	41692.39	0.03	0.04	41695.69	0.03	0.05	41697.87
0.04	0.01	41700.38	0.04	0.02	41702.75	0.04	0.03	41695.80	0.04	0.04	41697.38	0.04	0.05	41699.46
0.05	0.01	41696.69	0.05	0.02	41693.96	0.05	0.03	41691.87	0.05	0.04	41688.90	0.05	0.05	41694.52
$D^{max} = 0.01$; Two-point crossover ($P_c = 1$)														
0.005	0.01	41711.66	0.005	0.02	41709.06	0.005	0.03	41707.65	0.005	0.04	41703.69	0.005	0.05	41706.06
0.01	0.01	41708.72	0.01	0.02	41704.36	0.01	0.03	41701.20	0.01	0.04	41702.48	0.01	0.05	41705.04
0.02	0.01	41704.11	0.02	0.02	41703.81	0.02	0.03	41701.81	0.02	0.04	41700.11	0.02	0.05	41703.50
0.03	0.01	41702.18	0.03	0.02	41700.47	0.03	0.03	41698.70	0.03	0.04	41701.44	0.03	0.05	41701.44
0.04	0.01	41703.66	0.04	0.02	41701.22	0.04	0.03	41698.41	0.04	0.04	41699.46	0.04	0.05	41702.50
0.05	0.01	41701.43	0.05	0.02	41699.13	0.05	0.03	41697.22	0.05	0.04	41699.83	0.05	0.05	41701.44

Bold values indicate the selection of optimal parameters at minimum total production cost

Table 8 Comparison of statistical results with other methods for IEEE 57-bus system

Different models	Method	Minimum	Average	Worst	SD	ET(s)
M1	**SKH**	**41676.9152**	**41679.0443**	**41689.2076**	**3.6486**	**49.36**
	KH	**41681.3521**	**41687.1537**	**41700.5925**	**4.6814**	**45.21**
	GABC (Jadhav and Bamane 2016)	41684.2011	41686.7298	41689.5730	1.5814	–
	ARCBBO (Ramesh and Premalatha 2015)	41686	41718	41737	–	–
	TLBO (Jadhav and Bamane 2016)	41688.8512	41693.1552	41698.0085	–	–
	ABC (Rezaei Adaryani and Karami 2013)	41693.9589	–	–	–	–
	PSO (Jadhav and Bamane 2016)	41695.1483	41714.1392	41717.5173	12.99	–
	CSO (Jadhav and Bamane 2016)	41696.1767	41708.3916	41718.945	13.68	–
	ICA (Jadhav and Bamane 2016)	41709.7292	41712.6836	41715.6957	11.57	–
	GA (Jadhav and Bamane 2016)	41711.9365	41719.604	41734.1638	18.15	–
	MATPOWER (Zimmerman et al. 2011)	51,347.86	–	–	–	–
M2	**SKH**	**10.6877**	**11.1110**	**12.0016**	**0.4751**	**49.58**
	KH	**11.2158**	**12.0275**	**13.5281**	**0.6360**	**45.01**
M3	**SKH**	**0.2721**	**0.2760**	**0.2879**	**0.0046**	**50.23**
	KH	**0.2738**	**0.2803**	**0.2934**	**0.0065**	**46.48**
M4	**SKH**	**1.0800**	**1.0810**	**1.0835**	**0.0011**	**49.92**
	KH	**1.0811**	**1.0825**	**1.0868**	**0.0015**	**46.01**

G-best guided ABC (GABC); teaching learning based optimization (TLBO); cat swarm optimization (CSO); imperialist competitive algorithm (ICA)

objective functions M1 to M4 over 20 independent trials; from these results, it is observed that the proposed algorithm outperforms all the other algorithms presented in the literature. The optimal set of control variables obtained with various models along with TPC, APL, *L*-index and EP values for M1 to M4 are furnished in Table 9. The minimum and maximum load bus voltage magnitudes in all the models are depicted in Fig. 6, from where it is proved that the proposed algorithm is capable of handling all the voltage constraints within their allowable limits. The variations of the TPC over iterations for KH and SKH algorithms are illustrated in Fig. 7. It is proved that the SKH algorithm converged faster and achieved better optimal result as compared to the KH algorithm. Figure 8 assesses the percentage of TPC savings of the SKH algorithm in comparison with other methods reported in the literature, which clearly indicates that the SKH algorithm provides highest cost savings compared with the other methods. All the above-mentioned results reveal that the proposed algorithm is superior and effective to solve all the single-objective OPF problems.

5.4 Sensitivity analysis

Further, sensitivity analysis is also conducted using the proposed SKH algorithm with the best tuning parameters of objective function M1 for IEEE 14-bus, IEEE 30-bus and IEEE 57-bus systems. After setting the perturbation of $\pm 20\,\%$ in the tuning parameters giving better optimal value, the minimum, average and worst TPC values over 20 trials are given in Table 10. It is observed for IEEE 14-bus system, the maximum variations attained from the optimal TPC value 8080.7045 ($/h) are 0.0107, 0.0266 and 0.0441 % of minimum, average and worst TPC values, respectively. Similarly, for the IEEE 30-bus system, the maximum deviations achieved from the optimal TPC value 800.5141 ($/h) are 0.0125, 0.0301 and 0.0699 % of minimum, average and worst TPC values respectively. Moreover, for IEEE 57-bus system, the maximum variations obtained with respect to the optimal TPC value 41676.9152 ($/h) are 0.01, 0.0292 and 0.0488 % of minimum, average and worst TPC values, respectively. Hence, it can be identified that the obtained results are not much sensitive to the parameters variations.

6 Conclusion

Here, the new SKH algorithm is presented where the concept of SSC operator is augmented with the KH algorithm for improving the search process while solving the OPF problems. The SKH algorithm has been able to solve the OPF problems considering the minimization of total production cost, active power loss, *L*-index and emission pollution as objective functions. The most important privilege of the proposed SKH algorithm is obtaining better optimal solu-

Table 9 Optimal control variables for all models of IEEE 57-bus system

Control variables	M1	M2	M3	M4
P_{G1}(MW)	142.8235	200.9220	118.4496	236.9403
P_{G2}(MW)	90.4827	3.3270	99.9025	99.9999
P_{G3}(MW)	45.1846	139.9317	129.8141	140.0000
P_{G6}(MW)	71.8808	99.9470	83.1895	100.0000
P_{G8}(MW)	459.2338	307.3602	352.8545	291.9522
P_{G9}(MW)	96.1160	100.0000	99.9975	100.0000
P_{G12}(MW)	360.1577	409.9996	379.9074	298.2316
V_{G1}(p.u.)	1.0593	1.0023	1.0600	1.0520
V_{G2}(p.u.)	1.0575	0.9957	1.0566	1.0499
V_{G3}(p.u.)	1.0512	0.9987	1.0496	1.0406
V_{G6}(p.u.)	1.0594	0.9983	1.0581	1.0309
V_{G8}(p.u.)	1.0599	1.0012	1.0559	1.0293
V_{G9}(p.u.)	1.0373	0.9795	1.0417	1.0081
V_{G12}(p.u.)	1.0416	0.9855	1.0631	1.0106
t_{4-18}(p.u.)	0.9062	0.9643	0.9322	0.9039
t_{4-18}(p.u.)	1.0955	0.9004	1.0998	1.0093
t_{21-20}(p.u.)	1.0106	1.0096	1.0983	1.0137
t_{24-25}(p.u.)	0.9815	0.9759	1.0877	0.9668
t_{24-25}(p.u.)	1.0782	1.0312	0.9066	1.0203
t_{24-26}(p.u.)	1.0257	1.0021	0.9591	0.9999
t_{7-9}(p.u.)	0.9895	0.9327	1.0028	0.9624
t_{34-32}(p.u.)	0.9691	0.9493	0.9000	0.9529
t_{11-41}(p.u.)	0.9008	0.9004	0.9003	0.9000
t_{15-45}(p.u.)	0.9740	0.9176	0.9799	0.9584
t_{14-46}(p.u.)	0.9591	0.9059	0.9629	0.9420
t_{10-51}(p.u.)	0.9649	0.9172	0.9981	0.9430
t_{13-49}(p.u.)	0.9310	0.9001	0.9051	0.9191
t_{11-43}(p.u.)	0.9657	0.9026	0.9735	0.9360
t_{40-46}(p.u.)	0.9937	1.0000	1.0993	1.0023
t_{39-57}(p.u.)	0.9629	0.9776	1.0998	0.9624
t_{9-55}(p.u.)	0.9846	0.9263	0.9865	0.9469
b_{C18}(p.u.)	0.1580	0.0605	0.2529	0.0506
b_{C25}(p.u.)	0.1563	0.1399	0.1127	0.1281
b_{C53}(p.u.)	0.1380	0.1262	0.2627	0.1197
TPC ($/h)	**41676.9152**	45044.2407	43937.1058	45661.0588
APL (MW)	15.0795	**10.6877**	13.3154	16.3234
L-index	0.2807	0.2857	**0.2721**	0.2821
EP (ton/h)	1.9078	1.3937	1.2920	**1.0800**

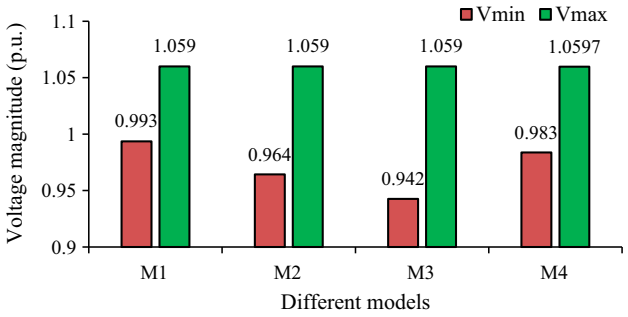

Fig. 6 Minimum and maximum load bus voltages of various models for IEEE 57-bus system

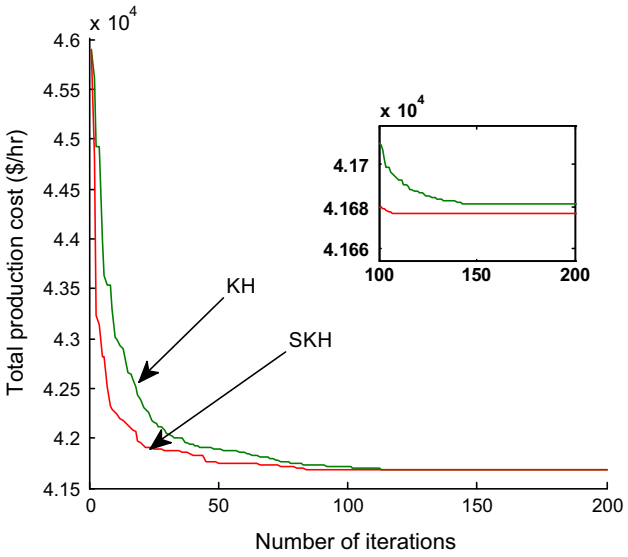

Fig. 7 Convergence characteristics with KH and SKH algorithms of M1 for IEEE 57-bus system

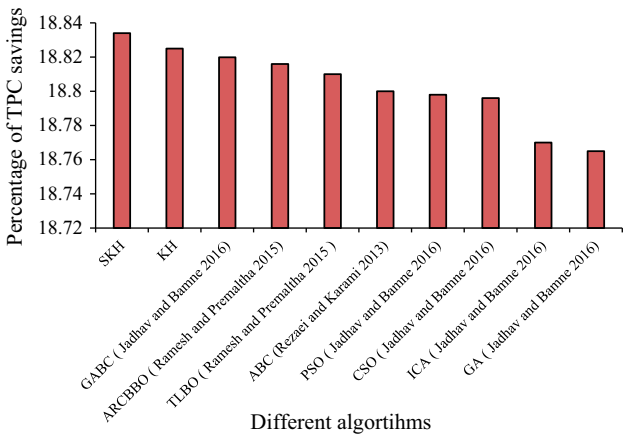

Fig. 8 Percentage of TPC savings of M1 for IEEE 57-bus system

tions in less number of iterations compared with the KH algorithm. The effectiveness and robustness of the SKH algorithm have been tested on IEEE 14-bus, IEEE 30-bus and IEEE 57-bus systems. The algorithm has been successful in producing feasible and optimal solutions for the standard test systems. The results obtained with the proposed SKH algorithm confirmed the good quality of different OPF solutions in comparison with the other algorithms in the literature.

Table 10 Results obtained with SKH perturbed parameters for IEEE 14-bus, IEEE 30-bus and IEEE 57-bus systems

Test System	Best Parameter - 20 %	Minimum Cost ($/h)	Average Cost ($/h)	Worst Cost ($/h)	Best Parameter + 20 %	Minimum Cost($/h)	Average Cost ($/h)	Worst Cost ($/h)
1	N^{max}	8081.0687 (0.0045 %)	8082.222 (0.0187 %)	8083.5236 (0.0348 %)	N^{max}	8080.9462 (0.003 %)	8081.9914 (0.0159 %)	8083.6271 (0.0361 %)
2		800.5268 (0.0015 %)	800.6592 (0.0181 %)	800.9441 (0.0537 %)		800.5446 (0.0038 %)	800.6704 (0.0195 %)	800.9856 (0.0589 %)
3		41677.67 (0.0025 %)	41687.45 (0.0252 %)	41693.92 (0.0408 %)		41679.5 (0.0063 %)	41686.7 (0.0234 %)	41692.8 (0.0382 %)
1	V_f	8080.9876 (0.0035 %)	8081.7352 (0.0127 %)	8083.7079 (0.0371 %)	V_f	8081.1738 (0.0058 %)	8082.2564 (0.0192 %)	8083.5421 (0.0351 %)
2		800.585 (0.0088 %)	800.6663 (0.0190 %)	801.023 (0.0636 %)		800.5579 (0.0054 %)	800.6515 (0.0181 %)	800.9870 (0.0590 %)
3		41678.75 (0.0043 %)	41686.3 (0.0225 %)	41692.03 (0.0362 %)		41678.38 (0.0035 %)	41688.37 (0.0274 %)	41696.64 (0.0473 %)
1	D^{max}	8081.1184 (0.0051 %)	8082.2429 (0.0190 %)	8083.6111 (0.0359 %)	D^{max}	8081.0205 (0.0039 %)	8082.0831 (0.0170 %)	8083.5041 (0.0346 %)
2		800.5326 (0.0023 %)	800.694 (0.0224 %)	800.9122 (0.0497 %)		800.6122 (0.0122 %)	800.7561 (0.0302 %)	800.9553 (0.0551 %)
3		41679.2 (0.0054 %)	**41689.1 (0.0292 %)**	41696.16 (0.0461 %)		41677.33 (0.0009 %)	41686.45 (0.0228 %)	41695.33 (0.0441 %)
1	N^{max}, V_f, D^{max} (All down)	8081.3004 (0.00785 %)	8082.4033 (0.0210 %)	8084.1057 (0.0420 %)	N^{max}, V_f, D^{max} (All up)	**8081.5706 (0.0107 %)**	**8082.8551 (0.0266 %)**	**8084.2595 (0.0441 %)**
2		800.5707 (0.0070 %)	800.6734 (0.0199 %)	801.0391 (0.0655 %)		**800.6149 (0.0125 %)**	**800.7555 (0.0301 %)**	**801.074 (0.0699 %)**
3		41679.57 (0.0063 %)	41687.64 (0.0257 %)	41695.1 (0.0436 %)		**41681.12 (0.0100 %)**	41688.25 (0.0271 %)	**41697.29 (0.0488 %)**

Compliance with ethical standards

Conflict of interest The authors declare that they have no conflict of interest.

Animal and human rights All procedures performed in studies involving human participants were in accordance with the ethical standards of the institutional and/or national research committee and with the 1964 Helsinki declaration and its later amendments or comparable ethical standards. This chapter does not contain any studies with animals performed by any of the authors.

Informed consent Informed consent was obtained from all individual participants included in the study.

References

Al-Rashidi MR, El-Hawary ME (2009) Applications of computational intelligence techniques for solving the revived optimal power flow problem. Electr Power Syst Res 79(4):694–702

Belgin ET, Rengin IC (2013) Optimal power flow solution using particle swarm optimization algorithm, In: Proceedings of the 15th international conference on computer as a tool (EUROCON-2013), Unska 3, Zagreb. doi:10.1109/EUROCON.2013.6625164

Celal Y, Serdar O (2011) A New hybrid approach for non-convex economic dispatch problem with valve-point effect. Energy 36:5838–5845

Dommel HW, Tinney WF (1968) Optimal power flow solutions. IEEE Trans Power Appar Syst 87(10):1866–1876

Frank S, Steponavice I, Rebennack S (2012) Optimal power flow: a bibliographic survey II, non-deterministic and hybrid methods. Energy Syst 3(3):259–289

Gaige W, Lihong G, Amir HG, Lihua C, Amir HA, Hong D, Jiang L (2013) Levy-flight krill herd algorithm. Math Prob Engg. doi:10.1155/2013/682073

Gai-Ge W, Amir HG, Amir HA (2013) A chaotic particle-swarm krill herd algorithm for global numerical optimization. Kybernetes 42(6):962–978

Gai-Ge W, Amir HG, Amir HA (2014a) An effective krill herd algorithm with migration operator in biogeography-based optimization. Appl Math Model 38:2454–2462

Gai-Ge W, Amir HG, Amir HA, Guo-Sheng H (2014b) Hybrid krill herd algorithm with differential evolution for global numerical optimization. Neural Comput Appl 25:297–308

Gai-Ge W, Gandomi AH, Alavi AH (2014c) Stud krill herd algorithm. Neurocomput 128:363–370

Gai-Ge W, Guo L, Wang H, Duan H, Liu L, Li J (2014) Incorporating mutation scheme into krill herd algorithm for global numerical optimization. Neural Comput Appl. doi:10.1007/s00521-012-1304-8

Gai-Ge W, Lihong G, Amir HG, Guo-Sheng H, Heqi W (2014e) Chaotic krill herd algorithm. Inf Sci 274:17–34

Gai-Ge W, Amir HG, Amir HA, Suash D (2015) A hybrid method based on krill herd and quantum-behaved particle swarm optimization. Neural Cromput Appl 27(4):989–1006

Gai-Ge W, Suash D, Amir HG, Amir HA (2016) Opposition-based krill herd algorithm with Cauchy mutation and position clamping. Neurocomput 177:147–157

Gandomi AH, Talatahari S, Tadbiri F, Alavi AH (2013) Krill herd algorithm for optimum design of truss structures. Int J Bio Inspired Comput 5(5):281–288

Gandomi AH, Alavi AH (2012) Krill herd: a new bio-inspired optimization algorithm. Commun Nonlinear Sci Numer Simul 17(12):4831–4845

Jadhav HT, Bamane PD (2016) Temperature dependent optimal power flow using g-best guided artificial bee colony algorithm. Int J Electr Power Energy Syst 77:77–90

Junpeng L, Yinggan T, Changchun H, Xinping G (2014) An improved krill herd algorithm: krill herd with linear decreasing step. Appl Math Model 234:356–367

Kessel P, Glavitsch H (1986) Estimating the voltage stability of a power system. IEEE Trans Power Deli PWRD-1. pp 346–354

Khatib W, Fleming P (1998) The stud GA: a mini revolution? 5th International Conference on Parallel Problem Solving from Nature. Springer, New York, pp 683–691

Lai LL, Ma JT, Yokoyama R, Zhao M (1997) Improved genetic algorithms for optimal power flow under both normal and contingent operation states. Int J Electr Power Energy Syst 19(5):287–292

Lihong G, Gai-Ge W, Amir HG, Amir HA, Hong D (2014) A new improved krill herd algorithm for global numerical optimization. Neurocomput 138:392–402

Ramesh KA, Premalatha L (2015) Optimal power flow for a deregulated power system using adaptive real coded biogeography-based optimization. Int J Electr Power Energy Syst 73:393–399

Reid GF, Hasdorf L (1973) Economic dispatch using quadratic programming. IEEE Trans Power Appar Syst 92:2015–2023

Rezaei Adaryani M, Karami A (2013) Artificial bee colony algorithm for solving multi-objective optimal power flow problem. Int J Electr Power Energy Syst 53:219–230

Sailaja Kunari M, Maheswarapu S (2010) Enhanced genetic algorithm based computation technique for multi-objective optimal power flow. Int J Electr Power Energy Syst 32(6):736–742

Sarat KM, Sudhansu KM (2015) Multi-objective economic emission dispatch solution using non-dominated sorting genetic algorithm-II. Discovery 47(219):121–126

Sayah S, Zehar K (2008) Modified differential evolution algorithm for optimal power flow with non-smooth cost functions. Energy Convers Manage 49:3036–3042

Shoults RR, Sun DT (1982) Optimal power flow based on P–Q decomposition. IEEE Trans Power Appar Syst 101:397–405

Sinsuphan N, Leeton U, Kulworawanichpong T (2013) Optimal power flow solution using improved harmony search method. Appl Soft Comput 13:2364–2374

Sun DI, Ashley B, Brewer B, Hughes A, Tinney WF (1984) Optimal power flow by newton approach. IEEE Trans Power Appar Syst 103:2864–2880

Tian Hao, Yuan Xiaohui, Huang Yuehua, Xiaotao Wu (2015) An improved gravitational search algorithm for solving short-term economic/environmental hydrothermal scheduling. Soft Comput 19:2783–2797

Torres GL, Quintana VH (1998) An interior-point method for nonlinear OPF using voltage rectangular coordinates. IEEE Trans Power Syst 13:1211–1218

Vaisakh K, Srinivas LR, Kala M (2013) Genetic evolving ant direction particle swarm optimization algorithm for optimal power flow with non-smooth cost functions and statistical analysis. Appl Soft Comput 13:4579–4593

Zehar K, Sayah S (2008) Optimal power flow with environmental constraint using a fast successive linear programming algorithm: application to the Algerian power system. Energy Convers Manage 49:3362–3366

Zimmerman RD, Murillo-Sanchez CE, Thomas RJ (2011) MATPOWER: steady-state operations, planning and analysis tools for power systems research and education. IEEE Trans Power Syst 26:12–19